Radio Interferometry: Theory, Techniques and Applications,
IAU Coll. 131, ASP Conference Series, Vol. 19, 1991,
T.J. Cornwell and R.A. Perley (eds.)

WIDE FIELD MAPPING OF 5C12

J.E. OKOPI and L.B. BÅÅTH

Onsala Space Observatory, S-439 00 Onsala, Sweden.

INTRODUCTION

The existing method of producing radio maps from interferometric data set is based on the assumption that there is a two dimensional fourier transform relationship between the sky brightness and the measured visibility. In mapping of a very wide field, this basic assumption breaks down due to various practical problems, e.g. bandwidth smearing. We present a wide-field mapping technique which is aimed at resolving some of these problems. This technique has been successfully applied to our MERLIN observations of the 5C12 region covering an area of 1800"x1800".

THE OBSERVATION AND MAPPING PROCEDURE

The observation was made with the MERLIN array in 1983 at 408 MHz, using the multichannel mode (20 channels). The MERLIN data were read into the astronomical image processing system (AIPS). The maps presented in this paper have been produced on the Convex C1 computer with AIPS. The mapping procedure is summarized below.

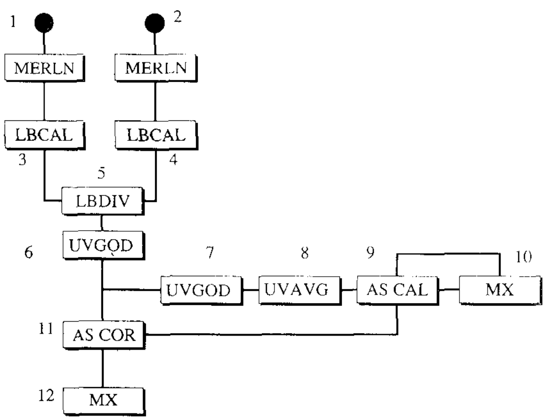

Fig. 1. 5C12 mapping sequence.

(1) Calibration source (0202+14R).
(2) MERLIN data.
(3) Calibrate (0202+14R) and (4) Calibrate MERLIN data.
(5) Correct bandpass with calibration source 0202+14R.
(6) Remove four noisy channels (1,2,19,20).
(7) Rotate to the reference source (5C12.216) and average in frequency.
(8) Average in time to reduce the number of visibility points.
(9) Do phase solution.
(10) Divide the whole field to 16 subfields, deconvolve with CLEAN and map.
(11) Apply solution to original data set.
(12) Map again. Repeat until final CLEAN maps are produced.

RESULT AND DISCUSSION

The resulting maps have a dynamic range of 1000:1. The position of the sources identified has good agreement with those in the Cambridge catalog (see TABLE I below).

TABLE I Source positions (Cambridge) and Flux density

Source	Positions $\alpha(1950.0)$	Positions $\delta(1950.0)$	Flux (mJy)
5C12.163	12 58 57.56	35 35 11.8	30
5C12.188	13 00 06.06	35 09 26.2	111
5C12.182	13 59 45.34	35 12 46.8	151
5C12.216	13 01 32.92	35 25 55.2	933
5C12.214	13 01 32.50	35 34 43.0	24
5C12.230	13 02 13.80	35 39 37.0	743
5C12.196	13 00 33.82	36 06 16.2	596
5C12.220	13 01 40.40	35 16 05.0	39
5C12.242	13 02 59.00	35 15 39.0	386
5C12.207	13 01 10.41	34 57 52.0	19
5C12.192	13 00 23.15	35 13 58.0	36
5C12.227	13 02 07.50	34 56 49.0	16
5C12.203	13 00 49.34	35 13 54.7	12
5C12.193	13 00 25.13	35 44 24.9	98
5C12.200	13 00 43.23	35 38 39.7	22
5C12.234	13 02 31.60	35 15 52.0	57

The effect of bandwidth smearing was resolved in stage 5 of our mapping procedure. However, the problem due to sky curvature still remains unsolved and it is reflected as elongated structures in some of the sources (e.g., 5C12.242 and 5C12.230) located far away from the reference source (5C12.216). The solution of this problem would require the development of a three-dimensional CLEAN algorithm. However, the computational effort and cost for such work would be very high.

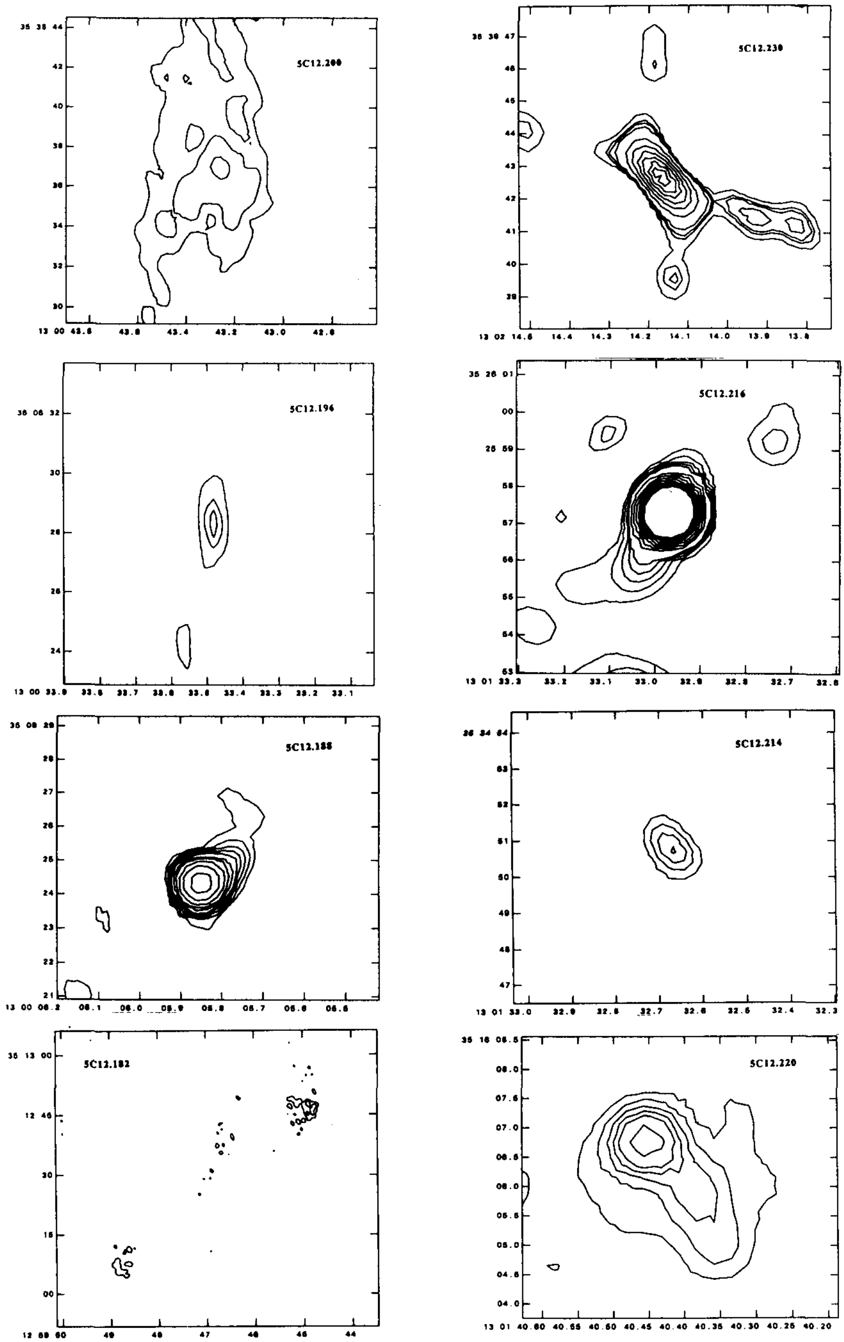

Fig. 2. 5C12 maps (X-axis is right ascension, Y-axis is declination)

https://doi.org/10.1017/S025292110010990X Published online by Cambridge University Press

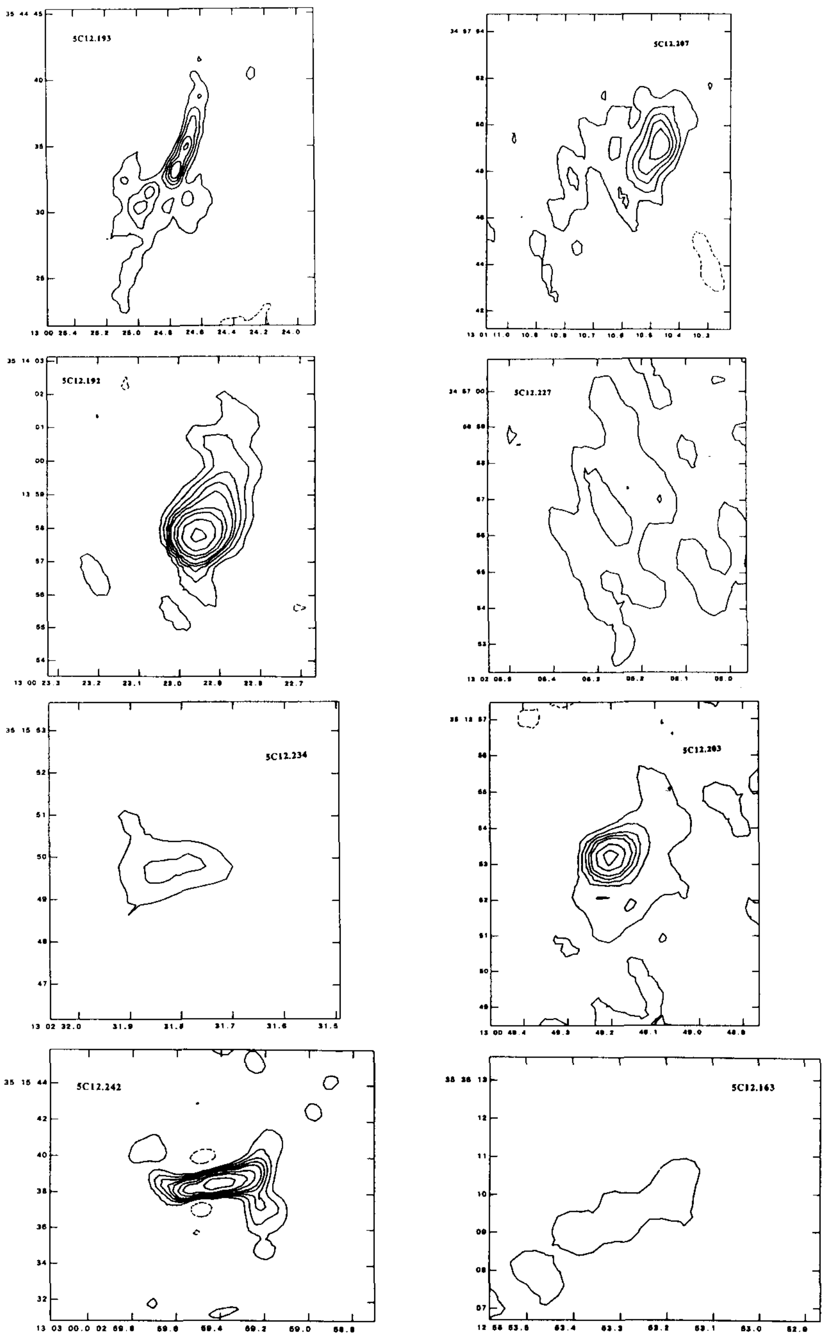

https://doi.org/10.1017/S025292110010990X Published online by Cambridge University Press